

Cite this: *RSC Advances*, 2012, 2, 11915–11921

www.rsc.org/advances

PAPER

Glucose/galactose/dextran-functionalized quantum dots, iron oxide and doped semiconductor nanoparticles with <100 nm hydrodynamic diameter†

SK Basiruddin, Amit Ranjan Maity and Nikhil R. Jana*

Received 5th September 2012, Accepted 10th October 2012

DOI: 10.1039/c2ra22055e

Cyanoborohydride based mild conjugation chemistry has been exploited for the covalent linkage between the reducing end of carbohydrates and primary amine terminated nanoparticles. The conjugation method has been extended to different nanoparticles such as quantum dots (QDs), iron oxide or doped semiconductor nanoparticles and different carbohydrates like maltose, lactose or dextran. Water soluble nanoparticles with a tunable surface charge and a hydrodynamic diameter between 20–100 nm have been synthesized that are terminated with glucose, galactose or dextrans of different molecular weights. Carbohydrate functionalized nanoparticles have been successfully used as nanoprobe for glycoprotein sensing and cellular targeting/imaging applications. The results show that carbohydrate functionalization offers enhanced labeling specificity and reduces the non-specific binding of nanoparticles.

Introduction

Functional nanoparticles are emerging as potential tools in biomedical applications.^{1–5} Nanoparticles are functionalized with various biomolecules like proteins, peptides, carbohydrates, lipids *etc.* and these nanobioconjugates are used in cellular and subcellular targeting, gene and drug delivery, therapy and diagnosis and in the study of various biological events *in vitro* and *in vivo*.^{1–5} Among various biomolecules, carbohydrates are particularly important.^{4–12} They are the most abundant biomolecules in the living body and are present in the form of glycoproteins, glycolipids and various other complex structures. They are present in cell membranes and the extracellular matrix and play an important role in cell–cell communication, cell signaling and metastatic cell growth. In addition, there are examples where carbohydrate based receptors are over expressed in certain cancer cells, and so can be used for selective cancer targeting and therapy.^{7–12} Thus, carbohydrate functionalized nanoprobe can be useful for specific targeting, detection, imaging and therapeutic applications.^{13–16}

Preparation of water soluble and colloiddally stable carbohydrate functionalized nanoparticles is very challenging because of the requirement of harsh conjugation chemistry, which may destabilize the nanoparticle structure, or specialized conjugation

approaches for different carbohydrates with a limited application potential.^{17–33} In earlier approaches, carbohydrates were attached to nanoparticles *via* the adsorption of thiolated carbohydrates^{17–21} or the covalent conjugation of functional group terminated nanoparticles with carbohydrates *via* EDC/DSC/DCC based conjugation,^{23–25} click chemistry,^{26,27} reductive amination based conjugation chemistry^{28–31} and other methods.^{32,33} Among them, the thiol based approach is most popular as it can produce monodispersed particles of small hydrodynamic diameter.^{17–21} However, this approach requires the synthesis of thiolated carbohydrates and stabilization of functional nanoparticles in physiological conditions is a critical issue³⁴ and dithiol/polythiol based carbohydrates are preferred for better capping with the nanoparticle.¹⁸ Other non-thiol based approaches are less popular due to multiple steps, the complexity associated with conjugation chemistry,^{5,26} poor conjugation efficiency,³¹ the destruction of the carbohydrate structure,³⁵ the large hydrodynamic diameter of the resultant particle³⁶ and limited colloidal stability of the final products.^{4,23} Thus, conjugation methods are highly desirable that can be used for different carbohydrates and nanoparticles, producing water soluble carbohydrate functionalized nanoparticles with hydrodynamic diameters <100 nm.

We worked on the development of bioimaging nanoprobe and reported various coating chemistries that can be used to transform as synthesized nanoparticles into different functional nanoparticles.³ These functional nanoparticles have 10–100 nm hydrodynamic diameter, a tunable surface charge, high colloidal stability in physiological conditions and optical/magnetic properties suitable for diagnostic applications. Herein we report a functionalization approach that can transform primary amine terminated nanoparticles into carbohydrate functionalized

Centre for Advanced Materials, Indian Association for the Cultivation of Science, Kolkata-700032, India. E-mail: camnrj@iacs.res.in; Fax: +91-33-24732805; Tel: +91-33-24734971

† Electronic supplementary information (ESI) available: Details of NMR and FTIR characterization of carbohydrate functionalized nanoparticles, experimental procedure of silica coating of QDs, carbohydrate functionalization using silica coated nanoparticles, details of the experimental procedure of biochemical activity tests using galactose/glucose/dextran functionalized QDs, more images of nanoparticle labeled cells, control cell labeling results and cytotoxicity study. See DOI: 10.1039/c2ra22055e

nanoparticles with good water solubility and colloidal stability. There are three distinct advantages of the presented carbohydrate functionalization approach over existing carbohydrate functionalizations with nanoparticles.⁴ First, linking occurs very selectively through the reducing end of the carbohydrates and the method is applicable to different carbohydrates that have reducing ends. Second, most of the nanoparticles survive in the functionalization conditions due to the mild conjugation chemistry and thus the method is applicable to different types of nanoparticles. Third, carbohydrate functionalized nanoparticles produced by this approach have a tunable surface charge and 20–100 nm hydrodynamic diameter, which are suitable for cellular and subcellular targeting and imaging applications. Following this method we have functionalized quantum dots (QDs), iron oxide and doped semiconductor nanoparticles with galactose, glucose and dextran of different molecular weights. We found that glucose/galactose functionalization offers selective binding with glycoproteins and specific cellular labeling and dextran functionalization reduces the non-specific binding property of the nanoparticles.

Experimental section

Chemicals and reagents

Maltose, lactose, dextran (MW 1000 and 6000), Igepal CO-520, poly(ethylene glycol) methacrylate (Mn \approx 360), *N,N'*-methylenebisacrylamide, 3-sulfopropylmethacrylate potassium salt, fluorescein-*o*-methacrylate, ammonium persulfate, 3-mercaptopropyltrimethoxysilane (MPS), [3-(2-aminoethylamino)propyl]trimethoxysilane (AEAPS), sodium cyanoborohydride [Na(CN)BH₃], dialysis membrane (MWCO 12–14 kDa), microcentrifuge filters (MWCO 30 kDa), concanavalin A (Con A), ricinus communis agglutinin 120 (RCA₁₂₀) and bovine serum albumin (BSA) were purchased from Sigma-Aldrich and used as received. *N*-(3-Aminopropyl)-methacrylamide hydrochloride was purchased from Polysciences and *N,N,N',N'*-tetramethylethylenediamine was purchased from Alfa Aesar.

Preparation of primary amine terminated nanoparticles

Hydrophobic ZnS capped CdSe based QDs,³⁷ λ -Fe₂O₃ based iron oxide nanoparticles³⁸ and Mn doped ZnS nanoparticles (Mn–ZnS)³⁹ were synthesized by standard organometallic approaches reported earlier. Next, these hydrophobic particles were converted into polyacrylate coated water soluble nanoparticles using a reverse micelle based approach reported earlier.^{37,40} In a typical synthesis hydrophobic nanoparticles were dissolved in reverse micelles, mixed with the desired acrylate monomer or monomer mixture and polymerization was initiated in nitrogen atmosphere by a persulfate initiator. In the present case we have used four acrylates; *N*-(3-aminopropyl)-methacrylamide that provides a primary amine and a cationic surface charge, 3-sulfopropylmethacrylate that provides an anionic surface charge, poly(ethylene glycol) methacrylate that provides a PEGylated surface and fluorescein-*o*-methacrylate that provides fluorescein incorporation into the polyacrylate backbone (used for iron oxide coating). In all cases \sim 5 mole percent methylenebisacrylamide was used to cross-link the polyacrylate shell. After one hour of reaction, the polyacrylate coated

nanoparticles were separated by ethanol addition, washed thoroughly and finally dissolved in water. The resultant polymer coated nanoparticles were terminated with primary amine, sulfopropyl or amine–sulfopropyl with different ratios; providing a cationic, anionic or zwitterionic surface charge, respectively.

Preparation of carbohydrate functionalized nanoparticles by cyanoborohydride based conjugation chemistry

2 mL of the polymer coated nanoparticle (absorbance \sim 0.5 at longest wavelength or 5 mg mL^{−1} for iron oxide) was taken in a 5 mL reaction flask and the solution pH was adjusted to pH 9 by adding a borate buffer. Next, 10–12 mg solid maltose/lactose/dextran was thoroughly mixed followed by the addition of 50–60 mg solid Na(CN)BH₃ and the solution was kept under magnetic stirring. The reaction was continued overnight. Next, the carbohydrate functionalized nanoparticle solution was purified from excess reagents either by dialysis or *via* microcentrifuge filtration. Typically, functionalized nanoparticles were dialyzed against a 12–14 kDa molecular weight cut off membrane for removing excess maltose/lactose and other reagents. Free dextran was removed from the dextran functionalized nanoparticles *via* microcentrifuge filtration (MWCO 30 kDa).

Cell culture and cell labeling

The HeLa and HepG2 cell lines, grown in a tissue culture flask, were subcultured in 24 well plates with 0.5 mL Dulbecco's Modified Eagle's Medium (DMEM) having 10% (v/v) fetal bovine serum (FBS). The cells were adhered to the culture plate after overnight incubation. Next, 20–100 μ L of the nanoparticle solution was added to each well containing the cells and incubated for 1–3 h. After that the cells were washed twice with PBS buffer solution (pH 7.4) to remove any unbound particles. Finally, the cell culture medium was added and imaging was performed.

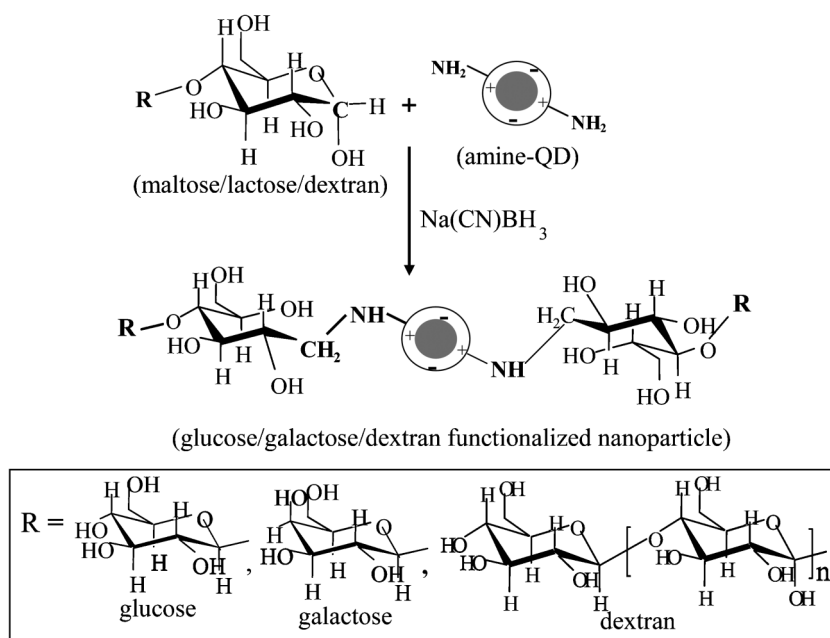
Instrumentation

All UV-visible spectra were measured on a Shimadzu UV-2550 UV-visible spectrophotometer using a quartz cell of 1 cm path length. Fluorescence spectra were measured on a Fluoromax-4 spectrofluorometer (Horiba JobinYvon). The MTT assay was performed using a Synergy TM MX multi-mode microplate reader. NMR spectra were measured with an FTNMR Bruker (DPX-500 MHz) instrument. Cellular images were captured using an Olympus IX 81 with DP 70 digital camera. Dynamic light scattering (DLS) and zeta potential studies were performed using a model NanoZS (Malvern) instrument. Fourier transform infrared (FTIR) spectra were measured with a Nicolet 6700 FT-IR instrument (Thermo Scientific) using KBr plates.

Results

Carbohydrate functionalization of nanoparticles

The carbohydrate conjugation method involves two steps: first, preparation of the primary amine terminated nanoparticles; second, covalent conjugation between the reducing end of the carbohydrates and the primary amine group of the nanoparticles *via* cyanoborohydride based reductive amination (Scheme 1). In



Scheme 1 Synthetic approach for carbohydrate functionalization of nanoparticles. Primary amine terminated nanoparticles, derived from polyacrylate coating, are reacted with carbohydrates in the presence of cyanoborohydride that covalently links the reducing end of the carbohydrates with the nanoparticles.

a typical conjugation method, an aqueous solution of nanoparticles is mixed with the carbohydrates and cyanoborohydride and the reaction is left overnight. Next, the resultant functional nanoparticles are separated from the unbound carbohydrates *via* dialysis or microcentrifuge filtration. Primary amine terminated QDs, iron oxide and doped semiconductor nanoparticles have been synthesized by polyacrylate coating or silica coating (ESI†) and used for conjugation. However, we focus mainly on polyacrylate coating as this coating provides higher colloidal stability and the surface charge of the resultant functional nanoparticles can be easily controlled to cationic, anionic or zwitterionic. QDs, iron oxide and doped semiconductor nanoparticles have been selected for functionalization as they have a high potential as bioimaging nanoprobes.^{1,3,5}

We have selected four different types of carbohydrates such as maltose, lactose and dextran with molecular weights of 1000 and 6000. All these carbohydrates have one reducing end (an aldehyde group) that makes a cyclic ester with an adjacent alcohol group (Scheme 1). In the presence of cyanoborohydride the reducing end of the carbohydrate reacts with a primary amine, forms a C–N bond and results in glucose/galactose/dextran terminated nanoparticles. Conjugation of carbohydrates with nanoparticles has been verified by FTIR and NMR spectroscopy and signals due to the carbohydrate molecules have been observed even after extensive purification by dialysis/microcentrifuge filtration (ESI†). The FTIR study shows that rocking and the symmetry deformed vibration of –NH_3^+ becomes absent or weaker after carbohydrate functionalization. In addition, the peak at 1632 cm^{-1} due to the N–H bending vibration of the primary amine gets weaker and shifts to 1645 cm^{-1} after carbohydrate functionalization. These results suggest that –NH_2 groups at the nanoparticle surface react with carbohydrates. The signature of carbohydrates is also confirmed from the increase

of the C–H stretching intensity at 2928 cm^{-1} and the broadening of the stretching vibration of O–H at 3420 cm^{-1} . The NMR study also shows the signature of protons associated with the carbohydrate moiety with δ values between 3.25 to 4 and the absence of any peak at a δ value of 5.3 due to the reducing end ‘H’. These results also indicate the successful conjugation and absence of any free carbohydrate in the purified nanoparticles.

Fig. 1, Table 1 and the ESI† show the colloidal solutions, optical properties, surface charge and hydrodynamic diameter of different carbohydrate functionalized nanoparticles. All the functional nanoparticles have high colloidal stability in different buffer solutions and in cell culture media. All three nanoparticles retain their optical properties after carbohydrate functionalization; QDs and Mn–ZnS show a strong red emission and $\lambda\text{-Fe}_2\text{O}_3\text{-fluorescein}$ shows strong green emission, without significant loss of the fluorescence quantum yield (Fig. 1a,b). The surface charge of the functional nanoparticles can be positive, negative or zwitterionic depending on the acrylate monomers used during coating. Primary/secondary amines provide a cationic surface charge, sulfate provides an anionic surface charge and amine–sulfate provides a pH dependent cationic/anionic surface charge. The hydrodynamic diameter of functional nanoparticles varies between 20 to 100 nm that includes a 3–8 nm size inorganic core, 5–15 nm polyacrylate shell⁴⁰ and surface bound carbohydrates. It is also observed that the average hydrodynamic diameter increases from 50 nm to 65 nm as the surface group changes from glucose to dextrans.

Carbohydrate functionalized nanoparticles as biological probes

We have tested the potential of carbohydrate functionalized nanoparticles as biological labels. On testing, nanoparticles functionalized with glucose, galactose and dextran show interactions with

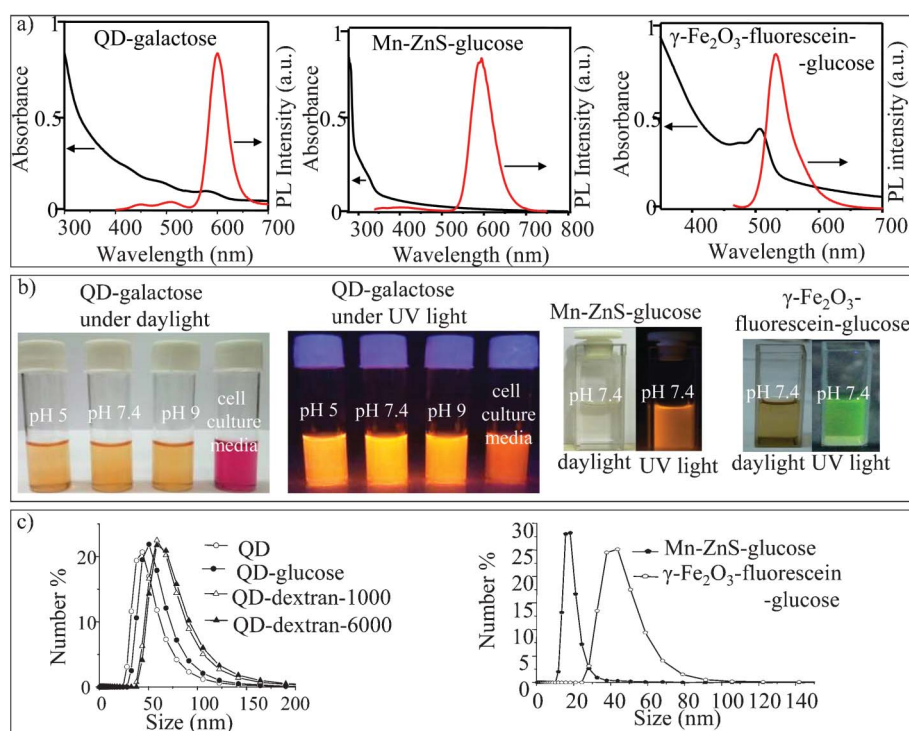


Fig. 1 (a) Absorption and emission spectra of different carbohydrate functionalized nanoparticles. (b) Digital images of solutions of carbohydrate functionalized nanoparticles in phosphate buffer solutions of different pH and in cell culture media. (c) Hydrodynamic diameter of nanoparticles after functionalization with different carbohydrate molecules, as observed from the dynamic light scattering study.

Table 1 Hydrodynamic size and surface charge of different carbohydrate functionalized nanoparticles

Nanoprobe	QD-glucose	QD-dextran-1000	QD-dextran-6000	Mn-ZnS-glucose	γ -Fe ₂ O ₃ -fluorescein-glucose	QD-galactose
Hydrodynamic diameter	50 ± 10 nm	60 ± 15 nm	65 ± 20 nm	20 ± 5 nm	40 ± 10 nm	45 ± 10 nm
Zeta potential (mV) at pH 5.0, 7.4, 9.0	+8, -4, -12	+11, 0, 0	+5, -3, -5	+12, -0, -11	+9, 0, -7	-17, -3, -17
Quantum Yield (%) ^a	7	7	7	3	21	7

^a Quantum yield of QDs and Mn-ZnS have been measured using quinine sulfate as the standard and the quantum yield of γ -Fe₂O₃-fluorescein has been measured using fluorescein as the standard.

glycoproteins that have a selective binding affinity to glucose/galactose and interactions with cells that have glucose/galactose receptors. Fig. 2a shows the results of the specific interaction between carbohydrate functionalized nanoparticles and glycoproteins. It shows that dextran or glucose functionalized nanoparticles bind to the glycoprotein concanavalin A (Con A) and leads to the visible precipitation of the nanoparticles from their solution. Similarly, galactose functionalized nanoparticles selectively bind to the ricinus communis agglutinin 120 (RCA₁₂₀) and lead to the visible aggregation of nanoparticles from their solution. The aggregation occurs due to the multiple binding sites present in the glycoproteins and nanoparticles that lead to cross-linking between nanoparticles (Fig. 2b). At pH 7 Con A has four binding sites for glucose and RCA₁₂₀ has two binding sites for galactose and each nanoparticle has more than one glucose/galactose on their surface. As a result the carbohydrate-glycoprotein interaction leads to cross-linking between nanoparticles. This type of aggregation is often observed for carbohydrate functionalized nanoparticles.²³ Control experiments show that polymer coated nanoparticles without any carbohydrate functionalization do not produce such

precipitates by adding glycoproteins. This result of the carbohydrate-glycoprotein binding interaction also proves that carbohydrates are successfully conjugated and retain their biochemical activity.

The effect of carbohydrate functionalization has been extensively investigated *via* cellular interaction and labeling studies. In this study we have used QD based nanoparticles as they offer easier fluorescence based detection and imaging of the labeled nanoparticles. Our results show two distinct conclusions. First, carbohydrate functionalization can decrease the non-specific binding of nanoparticles, particularly for the cationic nanoparticles. Second, carbohydrate functionalization offers an increased labeling selectivity of nanoparticles *via* a carbohydrate specific binding interaction. Fig. 3 shows images of HeLa cells labeled with QDs that are functionalized with glucose, dextran-1000 or dextran-6000. For this experiment the surface coating of the QDs is designed in such a way that it has both primary amine and sulfopropyl groups that result in solution pH dependent cationic or anionic surface charges due to protonation/deprotonation of the amine/sulfopropyl groups (Table 1). This coating

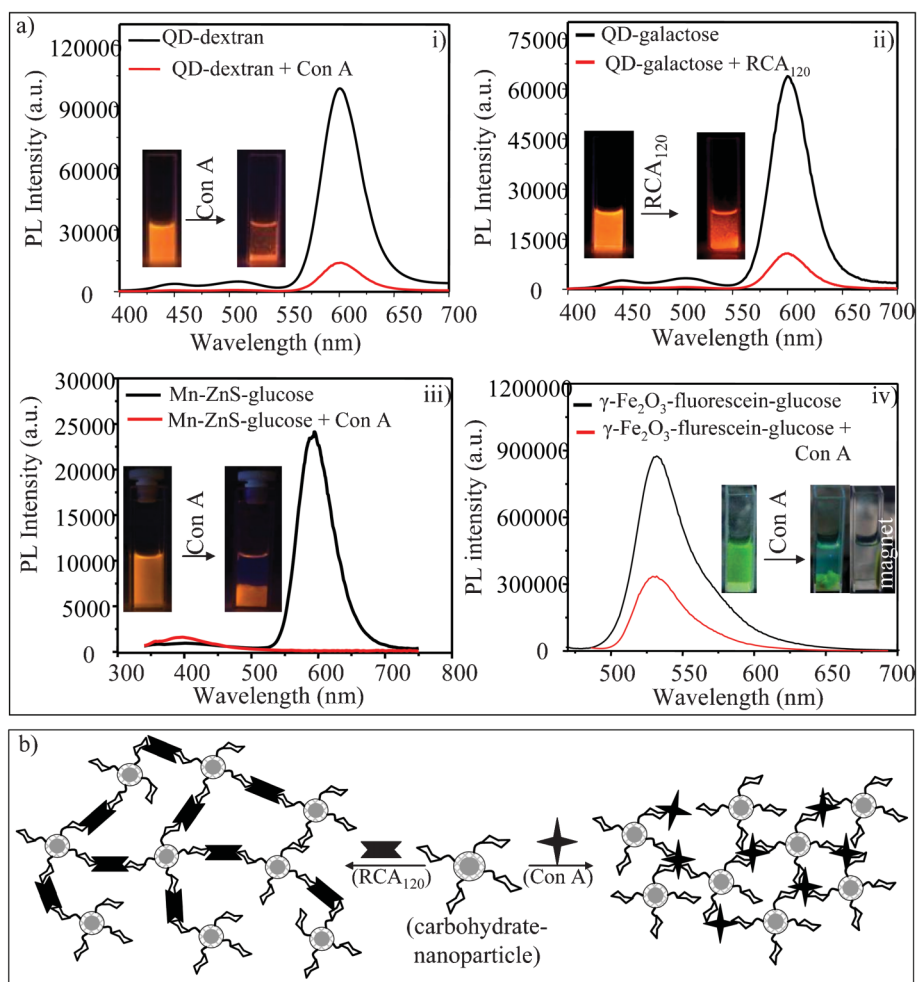


Fig. 2 (a) Biochemical activity test of different carbohydrate functionalized nanoparticles and (b) schematics showing the nanoparticle aggregation via a multivalent interaction between the functional nanoparticles and glycoproteins.

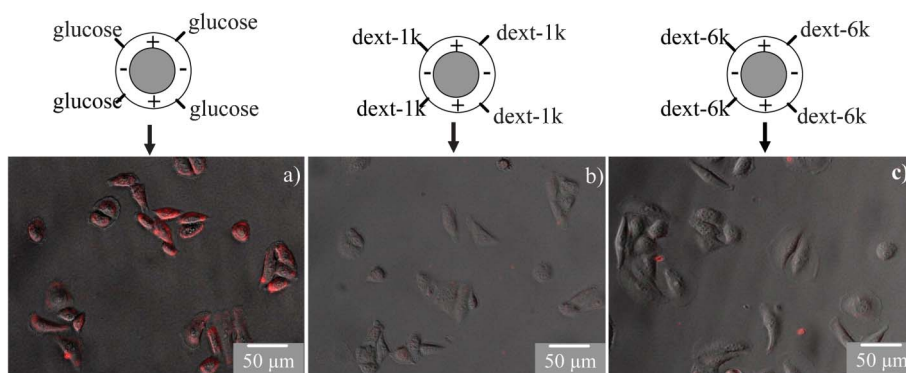


Fig. 3 Minimizing the non-specific cell labeling of QDs via carbohydrate functionalization. QDs are functionalized with glucose (a), dextran-1000 (dext-1k) (b) and dextran 6000 (dext-6k) (c). HeLa cells are used for the labeling study. Fluorescence images are combined with bright field images. The results show that non-specific cell labeling of QD-glucose is very high but is lowered for QD-dextran-1000 and QD-dextran-6000.

offers high non-specific binding to the cells. This is evident from the high labeling of glucose functionalized QDs by HeLa cells. However, this type of non-specific labeling/interaction is significantly lowered in dextran functionalized QDs and the effect is more prominent for dextran-6000 (Fig. 3). This result indicates that the dextran with a higher molecular weight is more

efficient in lowering the non-specific binding of the nanoparticles. The property of lowering the non-specific binding is often observed by polyethylene glycol functionalization of nanoparticles⁴¹ and was recently reported for glucose/galactose functionalized nanoparticles.⁴² The present result confirms earlier observations and shows that carbohydrates can also serve in

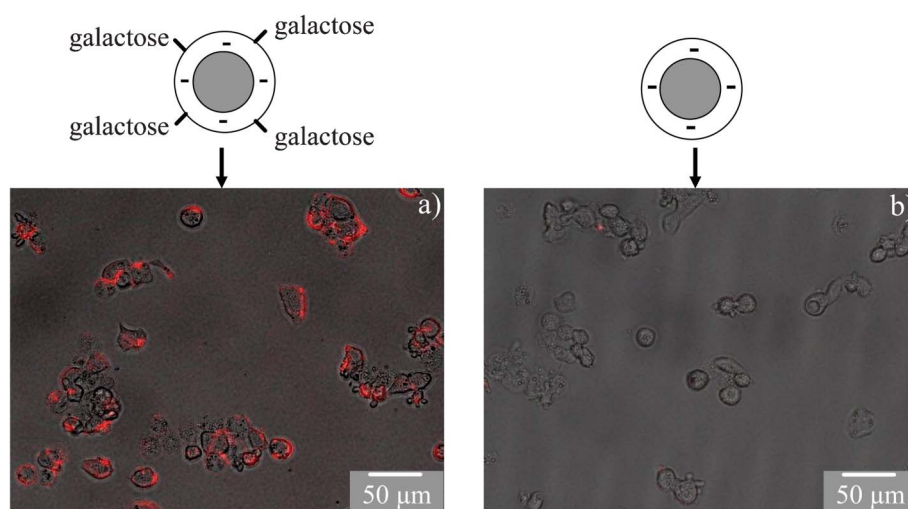


Fig. 4 Receptor mediated uptake of galactose functionalized QDs in HepG2 cells. Anionic QDs are used for galactose functionalization as they have a low cellular uptake. Fluorescence images are combined with bright field cell images. The results show high labeling of QD–galactose (a) as compared to QDs without any galactose functionalization (b).

lowering the non-specific binding of nanoparticles. Additionally, we found that higher molecular weights of carbohydrates are more effective in lowering the non-specific binding property.

The carbohydrate induced specific cell labeling of nanoparticles is shown in Fig. 4. In this experiment the surface charge of the QDs is intentionally selected as anionic so that it has a low nonspecific cellular interaction and labeling. The specific labeling and uptake of galactose functionalized QDs has been studied using HepG2 cells that have galactose specificialoglycoprotein receptors.¹⁸ The results show enhanced cellular labeling and uptake of galactose functionalized QDs through a receptor mediated interaction (Fig. 4 and ESI†). Control experiments show that QDs without any galactose functionalization or glucose functionalization do not label HepG2 (ESI†). Similarly, galactose functionalized QDs do not label HeLa cells as these cells do not have galactose receptors (ESI†). These results show that carbohydrate functionalized nanoparticles prepared in the present work can be used for selective cell labeling.

Discussion

Advantages and limitations of cyanoborohydride conjugation

Cyanoborohydride based reductive amination is an appealing approach as it uses mild reaction conditions and offers specific single point conjugation at the reducing end of carbohydrates. The mild reaction conditions preserve the structure and properties of the nanoparticles and single point conjugation preserves the carbohydrate structure. We have demonstrated that this approach can be applied to different nanoparticles (*e.g.* QDs, iron oxide and doped semiconductor nanoparticles) and different carbohydrate molecules (*e.g.* maltose, lactose and dextran). Currently different approaches are available to prepare primary amine terminated nanoparticles and many of the required carbohydrates are commercially available. Thus, the presented functionalization approach can be easily extended to other carbohydrates and nanoparticles.

Despite these advantages there are several limitations of this conjugation method. First, many sugars do not have a reducing

end and this method cannot be applied to them. Second, gold and silver nanoparticles are difficult to functionalize by this approach due to their reactivity with cyanoborohydride. We found that even in nitrogen atmosphere gold and silver nanoparticles dissolve under the present conjugation conditions. Traces of dissolved oxygen, longer reaction times and the high reactivity of Au/Ag in their nanoparticle form possibly contribute to this dissolution effect. Third, the conjugation requires excess carbohydrate and the removal of free carbohydrates. This is sometimes a difficult issue as some carbohydrates are very costly and the separation of high molecular weight carbohydrates requires a specialized approach (*e.g.* size exclusion chromatography).

Functional role of carbohydrates for nanoprobe

Earlier work shows that carbohydrate functionalization of nanoparticles offers binding selectivity in various biomedical applications. However, limited functionalization approaches restrict extensive studies on a wider size range of nanoparticles and for different carbohydrates.^{4,5,11} In contrast, the presented approach offers a wide range of carbohydrate functionalized nanoparticles having 20–100 nm hydrodynamic diameter and a tunable surface charge. This size range is optimum for *in vitro* and *in vivo* applications and the tunable surface charge can be used to optimize interaction with the bioenvironment.³ For example we have shown that the cellular interaction of 20–100 nm nanoprobe can be tuned by varying their surface charge or by varying the carbohydrate molecule on their surface. Our study shows two distinct functional roles of carbohydrates for the interaction of nanoprobe with the bioenvironment. First, carbohydrates can reduce the non-specific binding property of charged nanoparticles and thus indirectly enhance the labeling selectivity. For example we have shown that the high non-specific cellular interaction of cationic nanoprobe is reduced after dextran functionalization and this effect becomes significant once the molecular weight of the carbohydrates is >1 kD. Second, carbohydrates offer labeling selectivity *via* a specific

interaction with glycoprotein. The binding selectivity by carbohydrates is demonstrated *via* the specific interaction with proteins and cells. In reality carbohydrates exist in the form of macromolecules, polymers or nanoparticles with a tunable charge. Thus it is expected that in nanometer length scale, carbohydrates play these two roles separately or in combination in performing their biochemical activity.

Conclusion

We have used a cyanoborohydride based simple and mild conjugation approach that can transform primary amine terminated nanoparticles into carbohydrate functionalized nanoparticles. This conjugation method is unique as it covalently links the reducing end of the carbohydrate with the nanoparticles without destroying the carbohydrate and the method is applicable to different nanoparticles. Glucose, galactose and dextran functionalized nanoparticles have been synthesized that have 20–100 nm hydrodynamic diameter and high colloidal stability in physiological conditions. These carbohydrate functionalized nanoparticles are biochemically active and offer enhanced labeling specificity of nanoprobe with low non-specific binding. Compared to earlier reported methods the presented carbohydrate functionalization method is relatively simple, does not destroy the carbohydrates and produces robust functional nanoprobe.

Acknowledgements

The authors would like to thank DST and DBT, government of India for financial assistance. SB acknowledges CSIR, India for a research fellowship. ARM acknowledges DST and IACS, India for a research fellowship.

References

- 1 I. L. Medintz, H. T. Uyeda, E. R. Goldman and H. Mattoussi, *Nat. Mater.*, 2005, **4**, 435.
- 2 C. J. Murphy, A. M. Gole, J. W. Stone, E. C. Goldsmith and S. C. Baxter, *Acc. Chem. Res.*, 2008, **41**, 1721.
- 3 N. R. Jana, *Phys. Chem. Chem. Phys.*, 2011, **13**, 385.
- 4 X. Wang, O. Ramstrom and M. Yan, *Adv. Mater.*, 2010, **22**, 1946.
- 5 C. Tassa, S. Y. Shaw and R. Weissleder, *Acc. Chem. Res.*, 2011, **44**, 842.
- 6 P. G. Strange and D. E. Koshland, *Proc. Natl. Acad. Sci. U. S. A.*, 1976, **73**, 762.
- 7 O. Saitoh, W. C. Wang, R. Lotan and M. Fukuda, *J. Biol. Chem.*, 1992, **267**, 5700.
- 8 S. A. Brooks, D. M. S. Hall and I. Buley, *Br. J. Cancer*, 2001, **85**, 1014.
- 9 R. Kannagi, M. Izawa, T. Koike, K. Miyazaki and N. Kimura, *Cancer Sci.*, 2004, **95**, 377.
- 10 L. G. Yu, *Glycoconjugate J.*, 2007, **24**, 411.
- 11 P. H. Seeberger and D. B. Werz, *Nature*, 2007, **446**, 1046.
- 12 N. X. Arndt, J. Tiralongo, P. D. Madge, M. von Itzstein and C. J. Day, *J. Cell. Biochem.*, 2011, **112**, 2230.
- 13 Y. N. Zhao, B. G. Trewyn, I. I. Slowing and V. S. Y. Lin, *J. Am. Chem. Soc.*, 2009, **131**, 8398.
- 14 K. S. Kim, W. Hur, S. J. Park, S. W. Hong, J. E. Choi, E. J. Goh, S. K. Yoon and S. K. Hahn, *ACS Nano*, 2010, **4**, 3005.
- 15 L. N. Cui, J. A. Cohen, K. E. Broaders, T. T. Beaudette and J. M. J. Frechet, *Bioconjugate Chem.*, 2011, **22**, 949.
- 16 M. Gary-Bobo, Y. Mir, C. Rouxel, D. Brevet, I. Basile, M. Maynadier, O. Vaillant, O. Mongin, M. Blanchard-Desce, A. Morere, M. Garcia, J. Durand and L. Raehm, *Angew. Chem., Int. Ed.*, 2011, **50**, 11425.
- 17 H. Otsuka, Y. Akiyama, Y. Nagasaki and K. Kataoka, *J. Am. Chem. Soc.*, 2001, **123**, 8226.
- 18 R. Kikkeri, B. Lepenies, A. Adibekian, P. Laurino and P. H. Seeberger, *J. Am. Chem. Soc.*, 2009, **131**, 2110.
- 19 R. Wilson, D. G. Spiller, A. Beckett, I. A. Prior and V. See, *Chem. Mater.*, 2010, **22**, 6361.
- 20 M. Yu, Y. Yang, R. C. Han, Q. Zheng, L. J. Wang, Y. K. Hong, Z. J. Li and Y. L. Sha, *Langmuir*, 2010, **26**, 8534.
- 21 T. Ohyanagi, N. Nagahori, K. Shimawaki, H. Hinou, T. Yamashita, A. Sasaki, T. Jin, T. Iwanaga, M. Kinjo and S. I. Nishimura, *J. Am. Chem. Soc.*, 2011, **133**, 12507.
- 22 A. Saha, S. Basiruddin, R. Sarkar, N. Pradhan and N. R. Jana, *J. Phys. Chem. C*, 2009, **113**, 18492.
- 23 C. Earhart, N. R. Jana, N. Erathodiyil and J. Y. Ying, *Langmuir*, 2008, **24**, 6215.
- 24 C. H. Lai, C. Y. Lin, H. T. Wu, H. S. Chan, Y. J. Chuang, C. T. Chen and C. C. Lin, *Adv. Funct. Mater.*, 2010, **20**, 3948.
- 25 A. P. Goodwin, S. M. Tabakman, K. Welsher, S. P. Sherlock, G. Prencipe and H. J. Dai, *J. Am. Chem. Soc.*, 2009, **131**, 289.
- 26 S. Srinivasachari, Y. M. Liu, G. D. Zhang, L. Prevette and T. M. Reineke, *J. Am. Chem. Soc.*, 2006, **128**, 8176.
- 27 K. El-Boubbou, D. C. Zhu, C. Vasileiou, B. Borhan, D. Prosperi and W. Li, *J. Am. Chem. Soc.*, 2010, **132**, 4490.
- 28 M. Yalpani and D. E. Brooks, *J. Polym. Sci., Polym. Chem. Ed.*, 1985, **23**, 1395.
- 29 Q. H. Zhao, I. Gottschalk, J. Carlsson, L. E. Arvidsson, S. Oscarsson, A. Medin, B. Ersson and J. C. Janson, *Bioconjugate Chem.*, 1997, **8**, 927.
- 30 S. S. Banerjee and D. H. Chen, *Chem. Mater.*, 2007, **19**, 6345.
- 31 J. C. Gildersleeve, O. Oyeleran, J. T. Simpson and B. Allred, *Bioconjugate Chem.*, 2008, **19**, 1485.
- 32 F. Osaki, T. Kanamori, S. Sando, T. Sera and Y. Aoyama, *J. Am. Chem. Soc.*, 2004, **126**, 6520.
- 33 T. T. Beaudette, J. A. Cohen, E. M. Bachelder, K. E. Broaders, J. L. Cohen, E. G. Engleman and J. M. J. Frechet, *J. Am. Chem. Soc.*, 2009, **131**, 10360.
- 34 J. Aldana, N. Lavelle, Y. J. Wang and X. G. Peng, *J. Am. Chem. Soc.*, 2005, **127**, 2496.
- 35 D. Miksa, E. R. Irish, D. Chen, R. J. Composto and D. M. Eckmann, *Biomacromolecules*, 2006, **7**, 557.
- 36 K. Babiuch, R. Wyrwa, K. Wagner, T. Seemann, S. Hoeppener, C. R. Becer, R. Linke, M. Gottschaldt, J. Weisser, M. Schnabelrauch and U. S. Schubert, *Biomacromolecules*, 2011, **12**, 681.
- 37 Y. F. Wei, N. R. Jana, S. J. Tan and J. Y. Ying, *Bioconjugate Chem.*, 2009, **20**, 1752.
- 38 N. R. Jana, Y. F. Chen and X. G. Peng, *Chem. Mater.*, 2004, **16**, 3931.
- 39 B. B. Srivastava, S. Jana, N. S. Karan, N. R. Jana, D. D. Sarma and N. Pradhan, *J. Phys. Chem. Lett.*, 2010, **1**, 454.
- 40 S. Basiruddin, A. Saha, R. Sarkar, M. Majumder and N. R. Jana, *Nanoscale*, 2010, **2**, 2561.
- 41 E. L. Bentzen, I. D. Tomlinson, J. Mason, P. Gresch, M. R. Warnement, D. Wright, E. Sanders-Bush, R. Blakely and S. J. Rosenthal, *Bioconjugate Chem.*, 2005, **16**, 1488.
- 42 M. Moros, B. Hernaez, E. Garet, J. T. Dias, B. Saez, V. Grazu, A. Gonzalez-Fernandez, C. Alonso and J. M. de la Fuente, *ACS Nano*, 2012, **6**, 1565.